

# Passively mode-locked III-V/silicon laser with continuous-wave optical injection

Yuanbing Cheng,<sup>1</sup> Xianshu Luo,<sup>2</sup> Junfeng Song,<sup>2</sup> Tsung-Yang Liow,<sup>2</sup>  
Guo-Qiang Lo,<sup>2</sup> Yulian Cao,<sup>1</sup> Xiaonan Hu,<sup>1</sup> Xiaohui Li,<sup>1</sup>  
Peng Huei Lim,<sup>3</sup> and Qi Jie Wang<sup>1,\*</sup>

<sup>1</sup> OPTIMUS, Photonics Center of Excellence, School of Electrical & Electronic Engineering, Nanyang Technological University, 50 Nanyang Ave, 639798, Singapore

<sup>2</sup> Institute of Microelectronics, Agency for Science, Technology and Research, 11 Science Park Road, 117685, Singapore

<sup>3</sup> DSO National Laboratory, 20 Science Park Drive, 118230, Singapore

\*qjwang@ntu.edu.sg

**Abstract:** We demonstrate electrically pumped two-section mode locked quantum well lasers emitting at the L-band of telecommunication wavelength on silicon utilizing die to wafer bonding techniques. The mode locked lasers generate pulses at a repetition frequency of 30 GHz with signal to noise ratio above 30 dB and 1 mW average output power per facet. Optical injection-locking scheme was used to improve the noise properties of the pulse trains of passively mode-locked laser. The phases of the mode-locked frequency comb are shown to be coherent with that of the master continuous-wave (CW) laser. The radio-frequency (RF)-line-width is reduced from 7.6 MHz to 150 kHz under CW optical injection. The corresponding pulse-to-pulse jitter and integrated RMS jitter are 29.7 fs/cycle and 1.0 ps, respectively. The experimental results demonstrate that optical injection can reduce the noise properties of the passively mode locked III-V/Si laser in terms of frequency linewidth and timing jitter, which makes the devices attractive for photonic analog-to-digital converters and clock generation and recovery.

©2015 Optical Society of America

**OCIS codes:** (140.5960) Semiconductor lasers; (250.5300) Photonic integrated circuits; (220.0220) Optical design and fabrication.

---

## References and links

1. E. R. H. Fuchs, R. E. Kirchain, and S. Liu, "The future of silicon photonics: Not so fast? Insights from 100G ethernet LAN transceivers," *J. Lightwave Technol.* **29**(15), 2319–2326 (2011).
2. R. Soref, "The past, present, and future of silicon photonics," *IEEE J. Sel. Top. Quantum Electron.* **12**(6), 1678–1687 (2006).
3. C. Gunn, "CMOS photonics for high-speed interconnects," *IEEE Micro* **26**(2), 58–66 (2006).
4. R. E. Camacho-Aguilera, Y. Cai, N. Patel, J. T. Bessette, M. Romagnoli, L. C. Kimerling, and J. Michel, "An electrically pumped germanium laser," *Opt. Express* **20**(10), 11316–11320 (2012).
5. F. G. Della Corte and S. Rao, "Use of amorphous silicon for active photonic devices," *IEEE Trans. Electron. Dev.* **60**(5), 1495–1505 (2013).
6. W. Sibbett, A. A. Lagatsky, and C. T. A. Brown, "The development and application of femtosecond laser systems," *Opt. Express* **20**(7), 6989–7001 (2012).
7. J. Luo, N. Calabretta, J. Parra-Cetina, S. Latkowski, R. Maldonado-Basilio, P. Landais, and H. J. S. Dorren, "320 Gb/s all-optical clock recovery and time de-multiplexing after transmission enabled by single quantum dash mode-locked laser," *Opt. Lett.* **38**(22), 4805–4808 (2013).
8. E. U. Rafailov, M. A. Cataluna, and W. Sibbett, "Mode-locked quantum-dot lasers," *Nat. Photonics* **1**(7), 395–401 (2007).
9. J. Reichert, M. Niering, R. Holzwarth, M. Weitz, T. Udem, and T. W. Hansch, "Phase coherent vacuum-ultraviolet to radio frequency comparison with a mode-locked laser," *Phys. Rev. Lett.* **84**(15), 3232–3235 (2000).

10. T. Habruseva, D. Arsenijevic, M. Kleinert, D. Bimberg, G. Huyet, and S. P. Hegarty, "Optimum phase noise reduction and repetition rate tuning in quantum-dot mode-locked lasers," *Appl. Phys. Lett.* **104**(2), 021112 (2014).
11. C. M. DePriest, T. Yilmaz, A. Braun, J. Abeles, and P. J. Delfyett, "High-quality photonic sampling streams from a semiconductor diode ring laser," *IEEE J. Quantum Electron.* **38**(4), 380–389 (2002).
12. H. J. Yang, D. Y. Zhao, S. Chuwongin, J. H. Seo, W. Q. Yang, Y. C. Shuai, J. Berggren, M. Hammar, Z. Q. Ma, and W. D. Zhou, "Transfer-printed stacked nanomembrane lasers on silicon," *Nat. Photonics* **6**(9), 617–620 (2012).
13. H. Y. Liu, T. Wang, Q. Jiang, R. Hogg, F. Tutu, F. Pozzi, and A. Seeds, "Long-wavelength InAs/GaAs quantum-dot laser diode monolithically grown on Ge substrate," *Nat. Photonics* **5**(7), 416–419 (2011).
14. D. Liang and J. E. Bowers, "Recent progress in lasers on silicon," *Nat. Photonics* **4**(8), 511–517 (2010).
15. T. Hong, G. Z. Ran, T. Chen, J. Q. Pan, W. X. Chen, Y. Wang, Y. B. Cheng, S. Liang, L. J. Zhao, L. Q. Yin, J. H. Zhang, W. Wang, and G. G. Qin, "A Selective-Area Metal Bonding InGaAsP–Si Laser," *IEEE Photon. Technol. Lett.* **22**(15), 1141–1143 (2010).
16. M. Lamponi, S. Keyvaninia, C. Jany, F. Poingt, F. Lelarge, G. de Valicourt, G. Roelkens, D. Van Thourhout, S. Messaoudene, J. M. Fedeli, and G. H. Duan, "Low-threshold heterogeneously integrated InP / SOI lasers with a double adiabatic taper coupler," *IEEE Photon. Technol. Lett.* **24**(1), 76–78 (2012).
17. B. R. Koch, A. W. Fang, O. Cohen, and J. E. Bowers, "Mode-locked silicon evanescent lasers," *Opt. Express* **15**(18), 11225–11233 (2007).
18. A. W. Fang, B. R. Koch, K. G. Gan, H. Park, R. Jones, O. Cohen, M. J. Paniccia, D. J. Blumenthal, and J. E. Bowers, "A racetrack mode-locked silicon evanescent laser," *Opt. Express* **16**(2), 1393–1398 (2008).
19. M. L. Davenport, Srinivasan, M. J. R. Heck, and J. E. Bowers, "A hybrid silicon/InP integrated all-passive feedback stabilized mode-locked laser," *Optical Fiber Communication Conference and Exposition (OFC)/National Fiber Optic Engineers Conference (NFOEC)*, Th3A.5 (2014).
20. B. W. Hakki and T. L. Paoli, "CW degradation at 300 K of GaAs double-heterostructure junction lasers," *J. Appl. Phys.* **44**(9), 4113–4119 (1973).
21. D. von der Linde, "Characterization of the noise in continuously operating mode-locked lasers," *Appl. Phys. B* **39**(4), 201–217 (1986).
22. D. J. Derickson, R. J. Helkey, A. Mar, J. R. Karin, J. G. Wasserbauer, and J. E. Bowers, "Short pulse generation using multisection mode-locked semiconductor lasers," *IEEE J. Quantum Electron.* **28**(10), 2186–2202 (1992).
23. M. Margalit, M. Orenstein, G. Eisenstein, and V. Mikhaelshvili, "Injection locking of an actively mode-locked semiconductor laser," *Opt. Lett.* **19**(24), 2125–2127 (1994).
24. N. Rebrowa, T. Habruseva, G. Huyet, and S. P. Hegarty, "Stabilization of a passively mode-locked laser by continuous wave optical injection," *Appl. Phys. Lett.* **97**(10), 101105 (2010).
25. F. Kefelian, S. O'Donoghue, M. T. Todaro, J. G. McInerney, and G. Huyet, "RF linewidth in monolithic passively mode locked semiconductor laser," *IEEE Photon. Technol. Lett.* **20**(16), 1405–1407 (2008).

## 1. Introduction

Silicon photonics is attracting a lot of attention due to the prospect of integration of compact and cost-effective photonic and microelectronic elements on a single chip [1–3]. Though state-of-the-art passive silicon waveguide circuits have been well developed, the silicon based light sources, especially silicon mode locked lasers (MLLs), are still a challenge in silicon photonics due to the indirect bandgap nature of silicon material [4,5]. Semiconductor MLLs are excellent candidates for generating ultra-short optical pulses at high repetition rate [6]. Optical frequency combs emitted by MLLs have high extinction ratios, low jitter, and low chirp, which can be utilized in a variety of applications including arbitrary waveform generation, optical clock generation and recovery, coherent communications systems, high-speed analog-to-digital conversion and optical time-division multiplexing etc [7–11].

Integration of MLLs on silicon is quite promising as it combines the low loss and low dispersion characteristics of silicon with high gain III-V material, thus the performance of MLLs can be further improved. Among different approaches in heterogeneous integration of III–V semiconductors with silicon [12–14], wafer bonding technique followed by InP substrate removal is one of the most promising methods, which provides a route toward wafer-scale processing of these III-V epitaxial layers. Important achievements have been made in the past on the heterogeneous integration of III–V on silicon using a molecular, metal or adhesive bonding approach [14–16]. For the mode locked lasers, MLLs with two-section and racetrack structure, have been reported, respectively [17–19]. Ion implantation was used to realize the confinement of current injection into the device, which greatly complicated the fabrication processes. The lasing threshold for the MLL occurred when the gain sections had

an injection current of approximately 196 mA. Hybrid mode-locking [17] with 40 GHz RF power up to 17 dBm or optical feedback [19] was used to reduce the phase noise and timing jitter of the devices. In this paper, we describe the realization of a two-section passively MLL on silicon with continuous wave optical injection-locking scheme without using high-speed electronics to improve the noise properties of the pulse trains of passively MLL. Narrow III–V waveguides in the 2–3  $\mu\text{m}$  range are fabricated for continuous wave operation. In addition, a shallow etched waveguide is used which greatly reduces the optical and electrical losses coming from the straight section, allowing a much lower threshold and optical injection locking. The proposed method has been demonstrated as a simple and effective technique to achieve MLLs without using high-speed electronics.

## 2. Device structure and fabrication

The fabricated device consists of a 1250  $\mu\text{m}$  long gain section and a 30–100  $\mu\text{m}$  long saturable absorber (SA), which are separated by a 20  $\mu\text{m}$  electrical isolation regions as shown in Fig. 1. The devices were fabricated with a III-V epitaxial wafer bonded on a silicon wafer through heterogeneous integration. The III-V epitaxial layer stack that is used consists of a 200 nm thick p-InGaAs contact layer, a 1.5  $\mu\text{m}$  p-InP cladding layer, a 160 nm thick AlGaInAs upper separate confinement heterostructure layer, eight strained AlGaInAs quantum wells (6 nm) separated by nine AlGaInAs barriers (10 nm) and a n-InP cladding layer (110 nm).

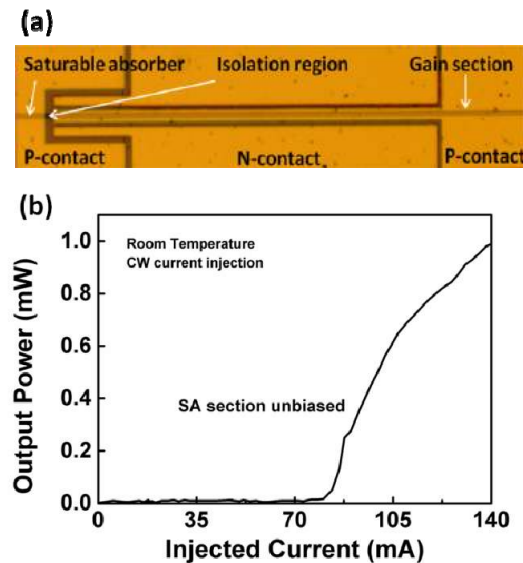


Fig. 1. (a) Diagram of the III-V/silicon MLL, (b) measured output power versus gain current where the SA is electrically open.

The heterogeneous integration is achieved by means of die-to-wafer bonding. Cleaved III-V pieces were bonded to a silicon substrate with a low temperature hydrophilic bonding process. In order to ease wafer-to-wafer bonding between III/V and silicon wafers, a cladding oxide is deposited first, and chemical mechanical polishing (CMP) is applied to planarize the wafer surface. The low-temperature bonding process starts from extremely thorough cleaning procedure for III-V die wafer and Si wafer in  $\text{NH}_4\text{OH}$  and  $\text{H}_2\text{SO}_4$ , respectively, followed by  $\text{O}_2$  plasma surface activation for 60 seconds, and deionized water rinse cleaning to terminate the surface with  $-\text{OH}$  groups. The bonded pairs are then placed into an EVG bonder with 1000 N mechanic force for 3 mins, followed with low temperature annealing at 300  $^\circ\text{C}$  for 15 hours. After wafer bonding and following InP substrate removal, a 2  $\mu\text{m}$ -wide shallow ridge is defined by  $\text{SiO}_2$  hard mask using the conventional contact lithography. Inductively coupled

plasma (ICP) etching is used to etch through the InGaAs layer and partly etch the p-doped InP layer with a  $\text{Cl}_2/\text{Ar}$  plasma, and then a selective wet etch is used to etch to the MQW layer. Subsequently, a second 12  $\mu\text{m}$ -wide deep ridge is formed by selectively wet etching through the MQW and the etching is stopped on top of the 110 nm InP n-contact layer. Electrical isolation between the gain and the SA sections is realized by forming 20- $\mu\text{m}$ -wide trench with depth of about 300 nm between them. An isolation resistance greater than 1 k $\Omega$  is obtained. Ti/Au metal stacks are deposited as contact metals for both p- and n-type contacts. Finally, the III-V/silicon wafer is cleaved after being thinned to 60  $\mu\text{m}$ , to form a Fabry-Pérot laser cavity. No coating is fabricated on the laser facets.

### 3. Experimental results and discussions

The device was measured at room temperature with a copper submount using an indium solder. The copper submount helps the thermal dissipation of the laser diode under operation. The laser optical output was collected by a photodiode located in front of the cleaved facet. It is found that the threshold current of the MLL becomes larger with longer SA. The device fails to lase when the length of SA section is above 60  $\mu\text{m}$  due to the high loss in the cavity. We select the MLL with a 50- $\mu\text{m}$ -long SA section for further measurement for achieving low threshold current and high output power. The typical threshold current with an unbiased 50- $\mu\text{m}$ -long SA section is 85 mA. The device has a maximum single facet continuous wave output power of 1 mW at room temperature when the injection current is 140 mA. The series resistance is about 8.5 Ohms, while the slope efficiency is 0.022 mW/mA. Optical spectrum at different injection currents is depicted in Fig. 2 (a), showing an optical emission centered at 1608 nm with a full-width at half-maximum (FWHM)  $\Delta\lambda$  of 0.8-nm at the injection current of 120 mA measured by an optical spectrum analyzer (OSA). The resolution of the OSA is 0.1 nm. Assume the generated optical pulse is chirped free (Fourier-transform-limited) and the shape of the pulse is with a  $\text{sech}^2$  function, the time-bandwidth product ( $TBP = \Delta\nu\Delta t$ ) is 0.3148 where  $\Delta t$  and  $\Delta\nu$  is the temporal and spectral FWHM of the pulse, respectively. The

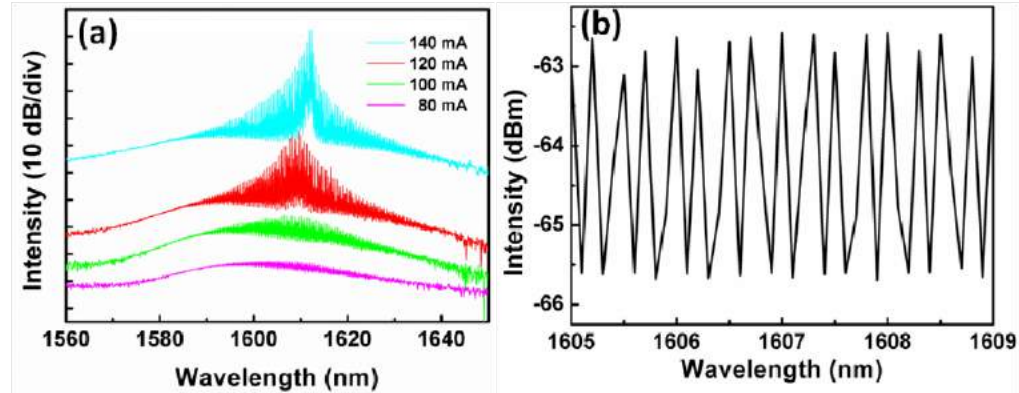


Fig. 2. (a) Optical spectra of the III-V/silicon MLL at different injection currents to the gain section while the SA section is floating, (b) the magnify image of the ASE spectrum of the device in the long wavelength range at the injection current of 80 mA.

temporal width of the optical pulse ( $\Delta t$ ) is calculated to 3.0 ps considering  $\Delta\nu = -\frac{\Delta\lambda}{\lambda^2}c$ , where  $\lambda$  and  $c$  denote the central optical wavelength of the device and the speed of light in vacuum, respectively. Waveguide losses of 13.9  $\text{cm}^{-1}$  were measured in the long wavelength range (1605 nm~1609 nm) from the amplified spontaneous emission (ASE) spectrum at the injection current of 80 mA which is below the threshold current as shown in Fig. 2 using the Hakki-Paoli technique [20]. Figure 2(b) depicts the magnification of the ASE

spectrum at 80 mA. The measured values of slope efficiency and modal loss (including waveguide loss and mirror loss) correspond to an internal quantum efficiency of 17.0%.

Passive ML of the device was obtained by forward biasing the gain section ( $I_{\text{gain}}$ ) and reverse biasing ( $V_{\text{sa}}$ ) or unbiasing the SA section. The ML behavior of the device was characterized in detail by measuring the radio frequency (RF) spectrum using spectrum analyzer (Agilent E4448A). Figure 3 shows the measured RF spectrum of the III-V/Si MLL at the injection current to the gain section ( $I_{\text{gain}}$ ) of 120 mA and unbiasing the SA section. The resolution bandwidth (RBW) during measurement is 3 MHz. The repetition frequency is about 30.0 GHz with signal to noise ratio above 30 dB and it can be tuned to more than 30 GHz by changing  $I_{\text{gain}}$ , giving clear evidence of passively mode locking of light signal. The measured 3dB RF linewidth of the mode locked laser was found to be 7.6 MHz from a Lorentzian fit of the RF spectrum centered at 30 GHz with a span of 100 MHz as shown in Fig. 3(b). For optimal mode locking, it is desirable for the saturation energy of the absorber to be much lower than that of the gain medium. Thus high reverse bias is desirable in the absorber and high gain currents are desirable in the gain region. However, self phase modulation (SPM) tends to occur in gain regions for pulses with high peak powers. This can lead to spectral broadening and chirping effect, which are not desirable for pulse transmission. The optimal condition of mode locking is  $I_{\text{gain}} = 120$  mA and  $V_{\text{sa}} = -0.5$  V, which leads to a RF linewidth of 7 MHz and signal to noise ratio of 35 dB.

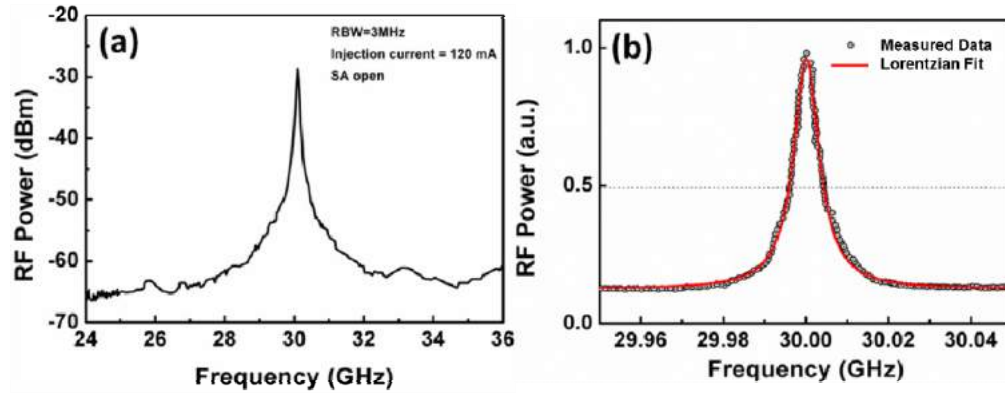


Fig. 3. (a) Measured RF spectrum of the III-V/Si MLL at  $I_{\text{gain}}$  of 120 mA and unbiasing the SA section. The RBW during measurement is 3 MHz. (b) measured RF spectrum (solid line/black) and its Lorentzian fit (dotted line/red) of the III-V/Si MLL at a frequency span of 100 MHz.

As mentioned above, MLLs with low noise are quite promising in the application of analog-to-digital conversion and optical communication. However, pulses generated by these lasers are affected by noise due to spontaneous emission and other factors such as cavity optical length fluctuations. In particular, their temporal positions in a pulse train deviate from those of the perfectly periodic output. This phenomenon called timing jitter limits the performance of mode-locked devices. The integrated root-mean-square (RMS) timing jitter of MLLs as a measurement of the phase noise can be calculated from the single-sideband (SSB) phase noise [21]

$$\sigma_{\text{RMS}} = \frac{1}{2\pi f} \sqrt{2 \int_{f_{\text{min}}}^{f_{\text{max}}} L(f) df} \quad (1)$$

where  $f$  is repetition frequency of the MLL,  $f_{\text{min}}$  and  $f_{\text{max}}$  determine the off-set frequency range over which the phase noise power spectral density  $L(f)$  is integrated. The RMS timing

jitter of our MLLs over the offset frequency range of 10 kHz to 100MHz is about 29.8 ps. This relatively large jitter value compared with conventional III-V two-section QW passively

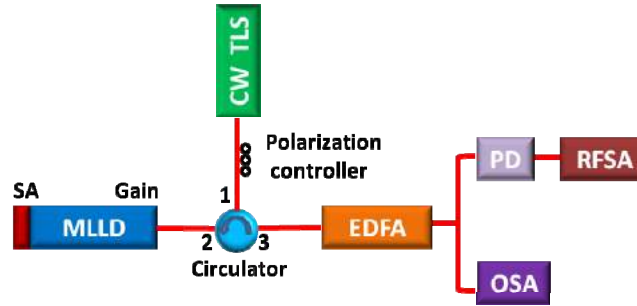


Fig. 4. Experimental setup for optical injection locking of the III-V/silicon MLL.

MLLs [22] is attributed to the large ASE noise, which may arise from the poor temperature characteristics of the hybrid laser due to the low thermal conductivity of  $\text{SiO}_2$  at the interface between III-V active layers and the silicon substrate, and the high internal loss of the cavity due to III-V layers' unique single separate confinement heterostructure structure.

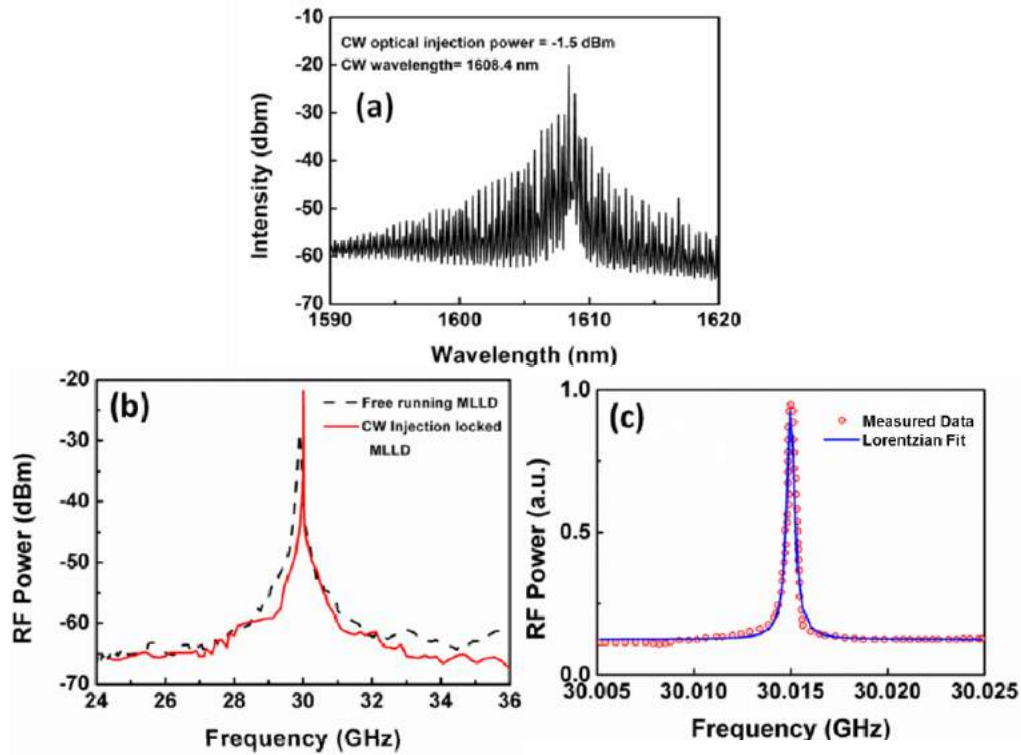


Fig. 5. (a) Optical spectrum of the III-V/silicon MLL under CW optical injection with injection optical power of  $-1.5$  dBm at  $1608.4$  nm, (b) measured RF spectrum of the free running (dashed line/black) and CW optically injected (solid line/red) III-V/Si MLL at  $I_{\text{gain}}$  of  $120$  mA, (c) measured RF spectrum (dotted line/red) and its Lorentzian fit (solid line/blue) of CW optical injected III-V/Si MLL at a frequency span of  $20$  MHz.

Optical injection locking has been shown to be a simple and effective technique to stabilize mode locked lasers without using high-speed electronics [23, 24]. This technique offers a large locking bandwidth whereas electronic phase-lock loops are limited by the



electrical bandwidth used and the inherent loop delay. The MLL's wavelength can be "pulled" toward the master wavelength, locking both its frequency and phase by optical injection locking. We use this optical injection technique to further reduce the time jitter of our III-V/Si MLLs. The optical injection locking was realized by injecting light from a linearly polarized CW single-mode tunable laser (Agilent 8164B) with narrow linewidth of 100 kHz into the cavity through the facet at the gain section. Figure 4 shows the experimental setup of master-slave configurations. The output of the circulator is sent to an Erbium doped fiber amplifier (EDFA, Photonik), which amplifies the signal (20 dB), so that it can be split to two ways with equal power: a 40GHz photodetector (PD) connected to a DC-50 GHz RF spectrum analyzer (RFSAs, Agilent E4448A), and an OSA. An optical circulator is used to ensure that only the output beam goes to the photodetector or SOA. The reflection style output is susceptible to reflected master light combining with the slave laser facet output. Figure 5(a) shows the corresponding optical and RF spectra of the MLL with CW optical injection power of  $-1.5$  dBm at the wavelength of 1608.4 nm. The input attenuation of the RF spectrum analyzer is set to 17 dB to exclude the amplification of EDFA (20 dB) and decrease due to optical splitter (3dB). The RBW during the frequency spectra measurement of the MLL under optical injection is 1 kHz. In the optical spectrum, we see that the injected mode had higher intensity than the other modes and the whole spectrum became narrower than free running. For comparison, we put the RF spectra of free-running and CW injected MLL together. As shown in Fig. 5 (b), the mode-locked peak shifted to higher frequency than that of the free running operation when locked to the master laser.

The 3dB RF linewidth of the injection locked laser was 150 kHz as found from a Lorentzian fit of the measured RF spectrum of the CW optical injected III-V/Si MLL with a span of 20 MHz as depicted in Fig. 5 (c), showing increased coherence of the locked mode.

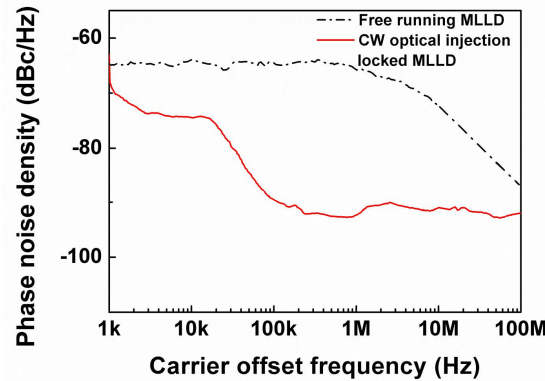


Fig. 6. Measured single sideband phase noise traces of the free running (dotted dash/black) and CW optical injected III-V/silicon MLL (solid line/red).

Also, an 8 dB increase in the peak of the RF frequency under optical injection is notable. The amplification of the mode-locked peak is believed due to the supermode noise reduction of the laser. The pulse to pulse timing jitter can be calculated as [25]

$$\sigma_{p-p} = \sqrt{\nu / 2\pi f^3} \quad (2)$$

where  $\nu$  denotes the 3-dB linewidth and  $f$  is repetition frequency of the MLL. The pulse-to-pulse jitters are reduced from 204.2 fs/cycle to 29.7 fs/cycle. Figure 6 shows representative single sideband phase noise traces for the free running and optical injection MLLs, respectively. Upon CW optical injection, the phase noise can be greatly reduced. The integrated RMS timing jitter of MLLs calculated from Eq. (1) is about 1.0 ps. Optical

injection therefore enables an alternative to hybrid mode-locking, particularly considering the major advantages of simplicity and low cost.

For mode locked laser, it is important that a low loss and high power output is achieved in the mode-locking situation. The main pulse broadening in mode locked laser occurs in the gain section due to gain saturation. Excess loss is introduced due to pulse shaping by self-phase modulation, and the net gain therefore also has to be increased. This leads to an increased spontaneous emission level which in turn results in more jitter. In order to improve MLL-performance, a high saturation energy in the gain section is desirable. One way to increase the gain saturation energy is to reduce the optical overlap of the waveguide mode with the active region. The methods such as large optical cavity structure and MLL with less numbers of QWs can be used to reduce the optical overlap of the waveguide mode with the active region. Other methods by including a long passive cavity or an active region with a flat gain spectrum in the laser structure can be used to further reduce the phase noise of MLLs in the next stage.

#### 4. Conclusion

In conclusion, electrically pumped mode locked quantum well lasers emitting at the L-band of telecommunication wavelength on silicon are demonstrated utilizing die to wafer bonding heterogeneous integration techniques. Narrow III–V waveguides in the range from 2 to 3  $\mu\text{m}$  are adopted for continuous wave operation. In addition, a shallow etched waveguide is used which greatly reduces the optical and electrical losses coming from the straight section, allowing a much lower threshold and optical injection locking. The mode locked lasers generate pulses at repetition frequency of 30 GHz with signal to noise ratio above 30 dB and 1 mW average output power per facet. Optical injection-locking scheme was used to improve the noise properties of the pulse trains of passively mode-locked laser. The 3dB RF linewidth is reduced from its original value to 150 kHz under CW optical injection. The corresponding pulse-to-pulse jitter and RMS jitter are 29.7 fs/cycle and 1.0 ps, respectively. The experimental results demonstrate that optical injection can reduce the noise properties of the passively mode locked III-V/Si laser in terms of frequency linewidth and timing jitter, which making the devices attractive for photonic analog-to-digital converters and clock generation and recovery. The proposed method has been demonstrated as a simple and effective technique to achieve low noise passively III-V/Si MLLs without using high-speed electronics.

#### Acknowledgments

This work is supported by A\*STAR SERC Future Data Center Technologies Thematic Strategic Research Programme under Grant No. 112 280 4038, and A\*STAR – MINDEF Science and Technology Joint Funding Programme under Grant No.122 331 0076.